# Fine Structure of Nearly Isotropic Bright Excitons in InP/ZnSe Colloidal Quantum Dots

Annalisa Brodu,[†,⊥] Vigneshwaran Chandrasekaran,[‡,¶,⊥] Lorenzo Scarpelli,[§] Jonathan Buhot,[‖] Francesco Masia,[§] Mariana V. Ballottin,[‖] Marion Severijnen,[‖] Mickaël D. Tessier,[‡,¶] Dorian Dupont,[‡,¶] Freddy T. Rabouw,[†] Peter C.M. Christianen,[‖] Celso de Mello Donega,[†] Daniël Vanmaekelbergh,[*,†] Wolfgang Langbein,[*,§] and Zeger Hens[*,‡,¶]

†*Debye Institute for Nanomaterials Science, Utrecht University, The Netherlands*

‡*Physics and Chemistry of Nanostructures, Ghent University, Ghent, Belgium*

¶*Center for Nano and Biophotonics, Ghent University, Belgium*

§*School of Physics and Astronomy, Cardiff University, Cardiff, United Kingdom*

‖*High Field Magnet Laboratory, HFML-EMFL, Radboud University, The Netherlands*

⊥*Contributed equally to this work*

E-mail: d.vanmaekelbergh@uu.nl; langbeinww@cardiff.ac.uk; zeger.hens@ugent.be

**Abstract**

The fine structure of exciton states in colloidal quantum dots (QDs) results from the compound effect of anisotropy and electron-hole exchange. By means of single-dot photoluminescence spectroscopy, we show that the emission of photo-excited InP/ZnSe QDs originates from radiative recombination of such fine-structure exciton states. Depending on the excitation power, we identify a bright exciton doublet, a trion singlet and a biexciton doublet line that all show a pronounced polarization. Fluorescence line

narrowing spectra of an ensemble of InP/ZnSe QDs in magnetic fields demonstrate that the bright exciton effectively consists of three states. The Zeeman splitting of these states is well described by an isotropic exciton model, where the fine structure is dominated by electron-hole exchange and shape anisotropy only leads to a minor splitting of the $F = 1$ triplet. We argue that excitons in InP-based QDs are nearly isotropic because the particular ratio of light and heavy hole masses in InP makes the exciton fine structure insensitive to shape anisotropy.

Colloidal quantum dots (QDs) are quasi-spherical semiconductor nanocrystals in which an electron-hole pair is confined in a volume with dimensions smaller than the exciton Bohr radius of the corresponding bulk material. Under such strong confinement conditions, the conduction- and valence-band edge are reduced to a set of quantized eigenstates that describe electron and hole motion. While these states can be calculated using different theoretical frameworks,[1–3] a multi-band effective mass approximation has the advantage of providing analytical expressions in which semiconductors are characterized by a limited set of parameters – which are often known for the corresponding bulk material – and the QD diameter is implemented as a continuously changing variable.[2] In the case of zinc blende or wurtzite semiconductors, which include II-VI and III-V materials such as CdSe, CdTe and InP, this approach leads to a two-fold degenerate lowest conduction-band state and a fourfold degenerate upper valence-band state.[2] As highlighted in Figure 1a-b, these degeneracies reflect the angular momentum of the Bloch states that make up the electron states at the edge of the conduction band ($s = 1/2$) and the valence band ($j = 3/2$), respectively.[2] The eigenstates of electron-hole pairs or excitons are then conveniently expressed using direct products of the two different conduction-band (electron) and four different valence-band (hole) states as a basis, see Figure 1c.

Quantum dots of both wurtzite and zinc blende semiconductors have a set of fine structure eigenstates with different eigenenergies that can be described by linear combinations of the 8 direct product exciton states. In the case of spherical zinc blende QDs, for example, the electron-hole exchange interaction splits the exciton levels in an optically dark low energy quintuplet and a high energy, bright triplet that are exciton eigenstates with total angular moment $F = j + s$ of 2 and 1, respectively (see Figure 1d). A further splitting of the exciton levels is obtained for QDs with an internal symmetry axis or quantization axis $z$, which can be the $c$-axis for QDs with the wurtzite structure or the rotation axis for QDs with a spheroidal shape. In such cases, 5 different fine structure levels are obtained, each characterized by a given projection $|F_z|$ along the quantization axis. Continuing with the example of a zinc

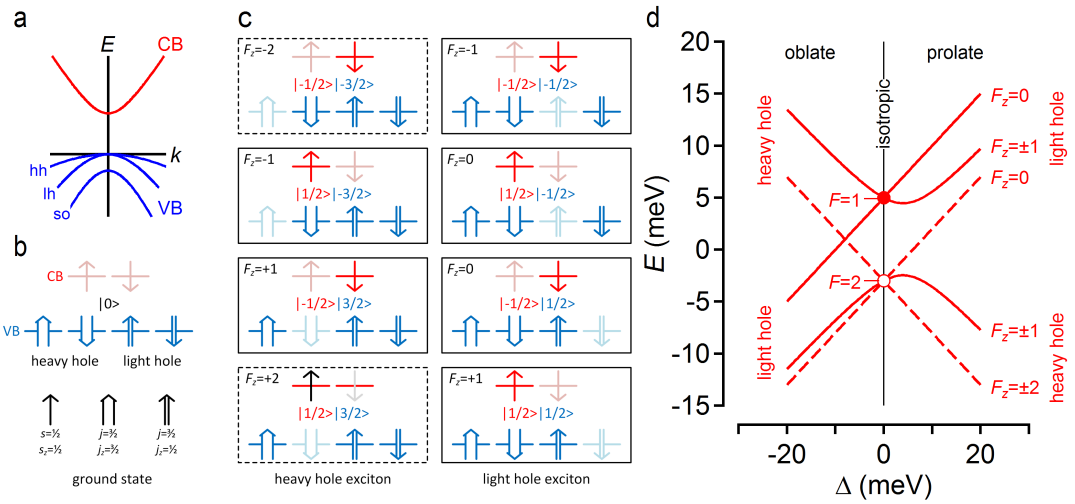


Figure 1: (a) Outline of the edges of (blue, VB) the valence-band and (red, CB) the conduction of a zinc blende semiconductor around the center of the Brillouin zone, showing the (lh) light hole, (hh) heavy hole and (so) split off VB. (b) Representation of the CB and VB Bloch states at the Γ point, highlighting the degeneracy of both states in relation to their $s = 1/2$ and $j = 3/2$ angular momentum. Bright colors represent occupied states, semi-transparent colors empty states. (c) Overview of the 8 exciton states obtained as direct products of a CB electron and a VB hole state. The direct product states are labeled using the $z$-component of the total angular momentum $F$ of the exciton. Transitions from the ground states to states boxed with a dashed line are spin forbidden. Again, bright colors represent occupied states and semi-transparent colors empty states. (d) Exciton eigenenergies calculated as a function of the anisotropy splitting energy Δ using an exchange splitting parameter $\eta = 2\,\mathrm{meV}$. States are labelled by means of the angular momentum projection quantum number $F_z$ along the quantization axis. Full lines represent bright states, dashed lines dark states. Note that exchange couples the two $F_z = 0$ states to yield a bright (singlet) state and a dark (triplet) state. In the isotropic case, only the three $F = 1$ states are bright, whereas the five $F = 2$ states are dark as indicated by the filled and open circles.

blende QD, shape anisotropy thus makes the subset of heavy hole or light hole excitons the lowest energy states, a situation typically seen with self-assembled QDs.[4] In either case, a dark exciton ground state is obtained, in combination with a twofold degenerate bright state at slightly higher energy, an energy difference often described as the dark-bright splitting.

For CdSe-based colloidal QDs, multiple studies have shown that the multi-band effective mass description of exciton states agrees with the experimental characteristics of these states. First, the observation that CdSe QDs exhibit longer radiative lifetimes at cryogenic temperatures, was assigned to the presence of a lowest energy dark exciton state.[5] Next, a

more detailed study interpreted the different exciton features visible through fluorescence line narrowing (FLN) and photoluminescence excitation spectroscopy using the combined contributions from electron-hole exchange, crystal and shape anisotropy to the exciton fine structure.[6] These reports were complemented by microphotoluminescence ($\mu$-PL) on single CdSe-based QDs, which confirmed the presence of a lowest dark state and allowed for a direct measurement of the dark-bright splitting from the respective emission lines.[7,8] More recently, this body of work was extended by the analysis of the emission of wurtzite CdSe QDs in magnetic fields, both at the level of ensembles and single QDs. These investigations highlighted the additional contribution of lateral shape anisotropy,[9,10] and resulted in estimates of the electron and hole $g$-factor.[11]

Importantly, restrictions on the use of Cd in consumer appliances have led researchers to investigate more recently InP-based QDs as a possible alternative to CdSe QDs. For InP QDs, however, the nature of the emissive state remains unclear. In line with the exciton model, time-resolved and fluorescence line narrowing photoluminescence studies confirmed the presence of a lowest energy dark state and a higher energy bright state, with a 5-10 meV dark-bright splitting,[12,13] Other reports, however, suggest that the photoluminescence may involve transitions between a conduction-band electron and a trapped hole.[14] In particular, a distribution of shallow hole traps may account for the persistently broad photoluminescence of InP QD ensembles and the remarkably large Stokes shift of the photoluminescence. On the other hand, studies using either photon-correlation Fourier spectroscopy in solution or $\mu$-PL have shown that single InP/ZnSe QDs have an emission line at room temperature that is $\sim 50$ meV wide, not unlike CdSe-based QDs.[15,16] Such discrepancies call for a more in-depth study on the InP QD fine structure, such that experimental data can be compared to predictions of the multiband effective mass model.

Here, we investigate the exciton fine structure of InP/ZnSe core/shell QDs by a combination of cryogenic single QD $\mu$-PL and FLN spectroscopy on QD ensembles in magnetic fields. We show that the emission spectrum of single InP/ZnSe QDs exhibits three characteristic

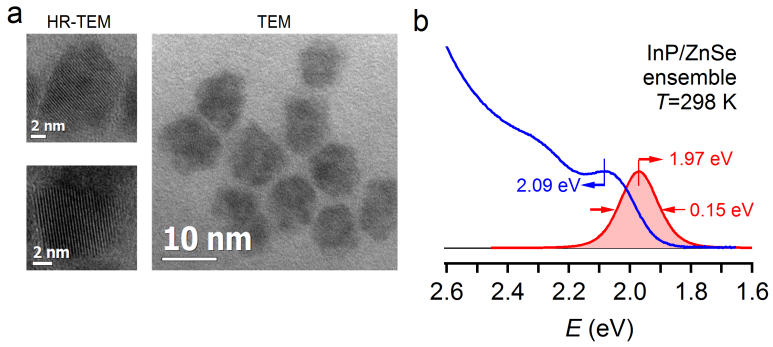


Figure 2: (a) Overview transmission electron microscopy (TEM) micrograph, showing InP/ZnSe QDs with a mean diameter of $10.2 \pm 0.9$ nm. (c) High resolution TEM micrograph, attesting to the crystallinity of the InP/ZnSe QDs used in this study. (b) Representation of (blue) absorption and (red) emission spectra of the ensemble of the InP/ZnSe QDs studied here.

features, which we assign to the bright exciton, trion and biexciton emission. For the example shown, the exciton and the biexciton appear as doublets split by $\sim 1$ meV, whereas the trion emission consists of a single line for which the phonon sidebands can be well resolved. Moreover, the polarization of the trion emission closely tracks that of the high energy line in the exciton doublet. While a bright doublet could result from lateral anisotropy in the $x-y$ plane,[9] which would split the bright $F_z = \pm 1$ level, the FLN spectra of InP/ZnSe QD ensembles show that the bright exciton consists effectively of 3 states that can be split by a magnetic field. This finding indicates that the bright exciton in InP/ZnSe QDs exhibits the fine structure of a nearly isotropic exciton that is split dominantly by electron/hole exchange and where the minor effect of shape anisotropy results in the bright, zero-field exciton doublet observed for single InP/ZnSe QDs.

For this study, we synthesized InP/ZnSe QDs according to the method proposed by Tessier *et al.*.[17] In brief, we reacted indium chloride and tris(di-ethylaminophosphine) in oleylamine to form InP QDs, which were shelled by ZnSe by adding zinc stearate and trioctylphosphine selenium to the reaction mixture (see Supporting Information S1). As shown in Figure 2a, this resulted in a dispersion of crystalline InP/ZnSe QDs featuring an overall diameter of $10.2 \pm 0.9$ nm. At room temperature, we retrieved the first exciton absorption

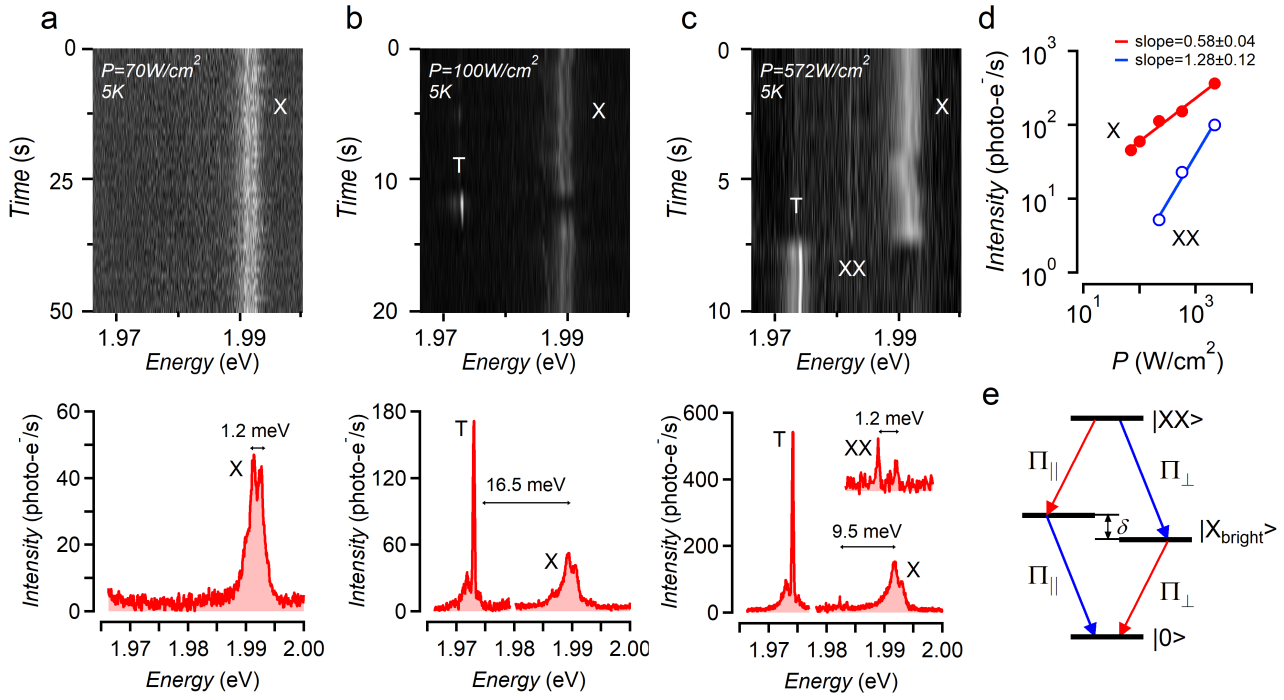


Figure 3: (a) (top) $\mu$-PL map recorded on a single InP/ZnSe core/shell QD at cryogenic temperatures (5 K) showing emitted intensity as a function of the photon energy and measurement time under low power excitation. A doublet emission feature labeled X is clearly visible. (bottom) Time integrated spectrum highlighting the spectral doublet and the energy splitting $\delta$ of 1.2 meV. (b) The same under higher excitation power, showing a temporal switch between the doublet X and a singlet emission line labeled T. Both features are retained in the integrated spectrum. (c) The same under even higher excitation power, showing a similar doublet-singlet switch as in (b) and the simultaneous occurrence of a second doublet labeled XX shifted by 9.5 meV to lower energy as compared to doublet X. (d) Integrated intensity of the X and XX doublets as a function of excitation power. (e) Scheme showing that in a biexciton-exciton-ground state emission cascade, the biexciton line and the exciton line will exhibit the same splitting.

maximum at 2.09 eV (594 nm) and the exciton emission at 1.97 eV (629 nm) with a linewidth of 150 meV, see Figure 2b. The photoluminescence quantum yield of the dispersed InP/ZnSe QDs studied here was determined at ~65%.

For single QD spectroscopy, we dropcast a nanomolar dispersion of InP/ZnSe QDs in a 1% solution of polystyrene-toluene on quartz coverslips, which was mounted in a PL microscope (see Supporting Information S2). Using continuous wave excitation at 473 nm while keeping the temperature set at 5 K, we observed various characteristic features in the emission spectrum of a single InP/ZnSe QD. At relatively low excitation power, the

image trace and the corresponding integrated spectrum feature a spectral doublet centered at 1.992eV and split by an energy difference of $\delta = 1.2$meV, see Figure 3a. Note that acoustic phonon sidebands (PSB) are visible on either side of the doublet line. Upon increasing the excitation power, the time trace represented in Figure 3b features an abrupt, temporal interruption of the doublet emission that leads to a single, narrow emission line 16.5 meV to the red of the doublet line. This singlet line exhibits clear phonon sidebands at either side of the central emission line. These sidebands account for 30% of the total emission and have a maximum intensity shifted by 1.1 meV with respect to the main emission line, an energy shift that agrees with the vibrational modes of small InP nanocrystals.[18] As outlined in Supporting Information S3, we estimate a sample temperature of 9 K from the intensity ratio of the Stokes and anti-Stokes emission bands. A similar switching between emission spectra characterized by a doublet line and a single line was observed in a $\mu$-PL study on CdSe/ZnS QDs by Fernee and coworkers.[19] Assigning the doublet to exciton emission and the singlet to trion emission, these authors interpreted the switching between the exciton and the trion emission to the random trapping of a band-edge carrier in a localized state.

Interestingly, at even higher power, the switching between the doublet at $\sim 1.992$ eV and the singlet line persists, yet the doublet line now concurs with a second, low-intensity doublet. This second doublet is shifted by 9.5 meV to lower energy and features the same splitting $\delta$ of 1.2 meV (see Figure 3c). Moreover, the intensity of the higher-energy doublet as recorded using continuous-wave excitation scales sub-linear with the excitation power, whereas the intensity of the additional, lower-energy doublet exhibits a supra-linear excitation power scaling. As indicated in see Figure 3d, fitting both power-dependent intensities to a power law yields two exponents with a ratio of $2.20 \pm 0.25$. Both observations support the assignment of the higher-energy doublet at $\sim 1.992$ eV to the bright exciton (X), and the lower energy doublet to the biexciton (XX). As outlined in Figure 3e, one indeed expects the transition from the biexciton to the exciton to yield an emission line that is the energetic mirror image of the bright exciton recombination. In that case, the singlet line can be assigned to a trion

transition (T), not unlike previous studies on single CdSe/ZnS QDs.[19] The exciton doublet of single CdSe/ZnS QDs, on the other hand, was interpreted in terms of the exciton dark-bright splitting, where the high energy line of the doublet corresponds to the bright exciton and the low energy line to the dark exciton recombination. However, in the case of InP/ZnSe QDs emitting at a similar photon energy as the QDs studied here, the dark exciton was only observed through a broad, phonon-coupled emission feature shifted 5-15 meV to the red of the bright exciton.[13] Clearly, this observation supports the assignment of the high energy doublet in the case of InP/ZnSe QDs to a bright exciton doublet rather than a bright-dark combination. Possibly, the combination of strong broadening and long radiative lifetimes makes the dark exciton indiscernible in the emission spectrum of single InP/ZnSe QDs. In addition, the competition between radiative recombination of the bright exciton and cooling into the dark exciton state may account for the lower than expected power scaling of the exciton and biexciton emission with increasing pump power since the presence of a dark exciton will promote non-radiative Auger recombination.

To corroborate the assignment of the three emission features to the exciton, the trion and the biexciton, we further analyzed the polarization of the different emission lines. To do so, we successively passed the emitted light through a rotatable half-wave plate and a calcite beam displacer separating the linearly polarized components along and orthogonal to the displacement. Both parts were transmitted through the input slit of an imaging spectrometer at different positions along the slit and detected by the same CCD camera. Figure 4a shows the thus recorded spectra $I_{\parallel}$ and $I_{\perp}$ for a fixed orientation of the half-wave plate – characterized by an angle $\theta$ and thus a polarization rotation $\phi = 2\theta$ – under excitation conditions where the X, T and XX emission features are present. One sees that all the emission lines exhibit a pronounced polarization. Interestingly, the polarization of the lines constituting the X and XX doublets are each others mirror image. As outline in Figure 3e, where the color coding agrees with the polarization analysis of 4a, this result is expected when both lines involve the same set of split bright exciton states. The trion

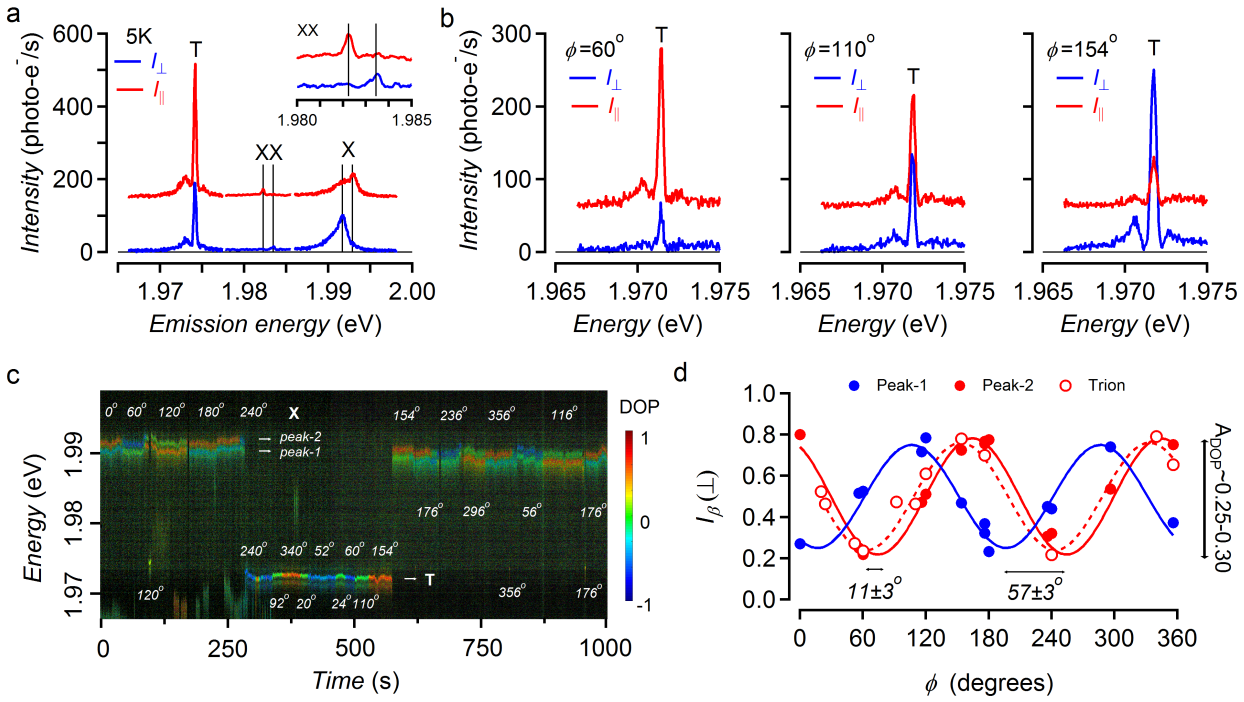


Figure 4: (a) Time-integrated emission spectrum of a single InP/ZnSe QD under excitation conditions that lead to exciton, trion and biexciton emission as recorded in (blue) the perpendicular and (red) the parallel channel. The inset shows a zoom on the biexciton doublet. For clarity, an offset of 150 photo-electrons/s was added to the parallel trace. (b) Zooms on the trion emission for different orientations of the half-wave plate as recorded in the perpendicular and parallel channel. The polarization rotation introduced by the half-wave plate is given by the angle $\phi = 2\theta$, where $\theta$ gives the rotation of the half-wave plate relative to a reference. (c) Color value/hue representation of the emission spectrum of a single InP/ZnSe as a function of time. The hue represents the degree of polarization as indicated, whereas the brightness (value) is proportional to the logarithm of the signal intensity. The indicated angles $\phi$ represent the temporary orientation of the half-wave plate as outlined above. (d) Relative intensity measured in the perpendicular channel as a function of the orientation of the half-wave plate for (filled blue dots) the low energy peak of the exciton doublet, (filled red circles) the high energy peak of the exciton doublet, and (open red circles) the trion. Lines represent best fits to Eq 2.

polarization, on the other hand, appears to coincide with that of the high energy line of the X doublet. Focusing on the trion line, Figure 4b highlights that the intensities measured in both channels systematically change while rotating the half-wave plate. Starting at $\phi = 60°$, the trion emission intensity is highest in the parallel channel. Upon rotating the half-wave plate to $\phi = 110°$, one sees that the intensities in both channels become about equal, while the highest intensity is recorded in the perpendicular channel at an angle $\phi = 154°$.

Using the intensity $I_{\parallel}$ and $I_{\perp}$ recorded in both channels, we can define a degree of polarization (DOP) as:

$$\mathrm{DOP} = \frac{I_{\parallel} - I_{\perp}}{I_{\parallel} + I_{\perp}} \tag{1}$$

Figure 4c shows an emission time trace recorded on the same InP/ZnSe QD as analyzed in Figure 3, but represented as a value/hue plot, where the color value and hue correspond to the total emission intensity and the DOP at each time point and emission energy. The figure highlights first of all the systematic difference in polarization of the two lines of the bright exciton doublet. Second, thanks to the switching between exciton and trion emission, it can be seen that the polarization of the trion indeed tracks the polarization of the high energy line of the exciton doublet. Both observations are confirmed in Figure 4d, which represents the relative intensity in the perpendicular channel for the two exciton lines and the trion as a function of the rotation induced by the half-wave plate. The full lines in Figure 4d represent fits of the different traces to the expression:

$$\frac{I_{\perp}}{I_{\parallel} + I_{\perp}} = \frac{1}{2} + A_{\mathrm{DOP}} \sin\left(2(\phi - \phi_0)\right) \tag{2}$$

As shown in Figure 4d, such fits yielded a DOP amplitude $A_{\mathrm{DOP}}$ in the range 0.25-0.3 for the different transitions. Moreover, the angular difference between the two lines of the exciton doublet amounted to $57 \pm 3°$, whereas the polarization angle of the triplet line and the high energy line of the exciton doublet was only shifted by $11 \pm 3°$.

As argued above, the observation that the PL of a single InP/ZnSe QDs randomly switches at high illumination power between a spectrum showing two doublet lines, commensurate in terms of energy splitting and polarization, and a singlet line indicate that this PL results from recombination of band-edge charge carriers rather than trapped carriers. The multiband effective mass model of the band-edge exciton fine structure provides two possible interpretations of a bright doublet in QDs with a zinc blende crystal structure. First, as shown in Figure 1d, pronounced shape anisotropy brings either the light hole or

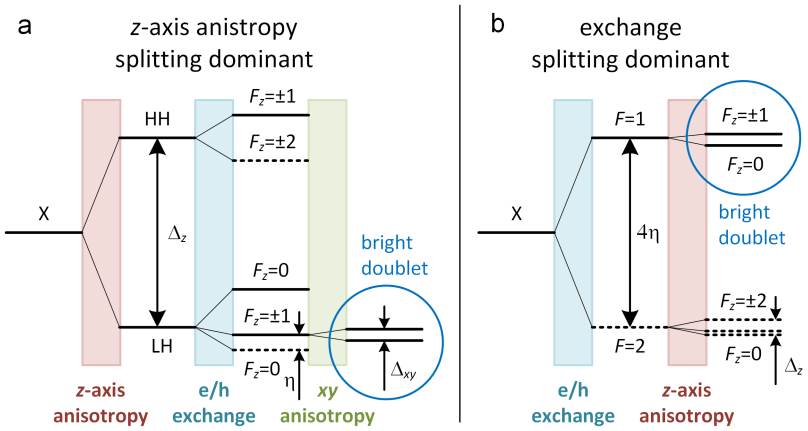


Figure 5: (a) Sequence of splitting of the exciton states when $z$ axis anisotropy dominates, for a case where the light hole exciton is lowered in energy. In that case, a bright exciton doublet can result from additional anisotropy in the $x-y$ plane. (b) Sequence of splitting of the exciton states when exchange dominates. In that case, a bright exciton doublet can result from a minor $z$-axis anisotropy. In both figures, $\eta$ is the exchange parameter and $\Delta$ the anisotropy energy for the ground state exciton,[20] whereas full lines represent bright exciton states and dashed lines are dark exciton states.

heavy hole exciton states down in energy, which are both 4-fold degenerate states that are further split by exchange interaction to give exciton states with a fixed component of the angular moment $F_z$ along the quantization axis $z$. This situation is detailed in Figure 5a for the case where the light hole is lowest in energy. This yields a fine structure in which a bright $F_z = \pm 1$ exciton doublet is separated from the $F_z = 0$ dark ground state by the exchange interaction and from the higher energy bright $F_z = 0$ exciton singlet by thrice the exchange interaction.[20] Additional anisotropy in the $xy$ plane will split this isolated $F_z = \pm 1$ exciton in two components,[9,10] emitting light linearly polarized along the $x$ and $y$ axis.[21] When the heavy hole states are lowest in energy, a similar situation arises where the lowest-energy bright state is an $F_z = \pm 1$ exciton that will be split by lateral anisotropy. Second, when the exchange interaction dominates, shape anisotropy will merely split the upper bright triplet in two components, a first with angular momentum $F_z = 0$ and a second with angular momentum $F_z = \pm 1$ (see Figure 5b). Such excitons will emit light linearly polarized along the $z$-axis and light circularly polarized within the $xy$ plane, respectively. Finally, while shape anisotropy makes the low energy $F_z = \pm 1$ exciton bright through coupling with the high

energy $F_z = \pm 1$ exciton, this effect remains negligible for small deviations from the isotropic case. Hence the representation of the lower energy $F_z = \pm 1$ exciton by a dashed line in Figure 5b.

To determine the overall degeneracy of the bright exciton – 2-fold with a minor splitting due to anisotropy in the $xy$ plane or 3-fold with a minor splitting due to anisotropy along the quantization axis $z$, see Figure 5 – we analyzed the emission of an ensemble of InP/ZnSe QDs by FLN spectroscopy in a magnetic field. For this study, a sample with a peak emission at 2.12 eV at 4 K was used (see Supporting Information S4), which we pumped resonantly at 2.06 eV using a monochromatic laser source. While not exactly identical, these experimental settings are in good correspondence with the single InP/ZnSe QDs discussed before. As outline in Supporting Information S4, FLN spectra were acquired in Faraday configuration with the excitation light parallel to the direction of the magnetic field. The excitation light had a $\sigma^+$ circular polarization, which dominantly excites the $F_z = +1$ state in the given configuration, while we detected emitted light with $\sigma^-$ polarization.

Figure 6a represents the FLN spectra acquired in the absence of a magnetic field using the excitation conditions described above. Note that we use the energy difference $\Delta E = \hbar\omega_{exc} - \hbar\omega_{em}$ between the excitation and emitted photons as the horizontal axis. The three broad features labelled C, D and E in the FLN spectrum were assigned previously to (C) the phonon activated dark exciton emission, and replicas of this transition involving the additional emission of (D) ZnSe or (E) InP LO phonons.[13] Using the latter two as a yardstick, we estimate the bright-dark splitting in these InP/ZnSe QDs at $\Delta E_{bd} = 6$ meV (see Figure 6a). In Figure 6b, we show the low energy part of various FLN spectra obtained on the same InP/ZnSe QD ensemble, while increasing the magnetic field from 10 to 30 T. Interestingly, we observe two additional features that shift to lower energy relative to the $F_z = +1$ state with increasing magnetic field. A first, labeled as A, can be discerned for fields of 18 T and higher and shifts from $\Delta E = 2.25$ meV to 3.58 meV at 30 T (see Supporting Information S4). A second, labeled B, appears first at fields of 10 T. This feature shifts more

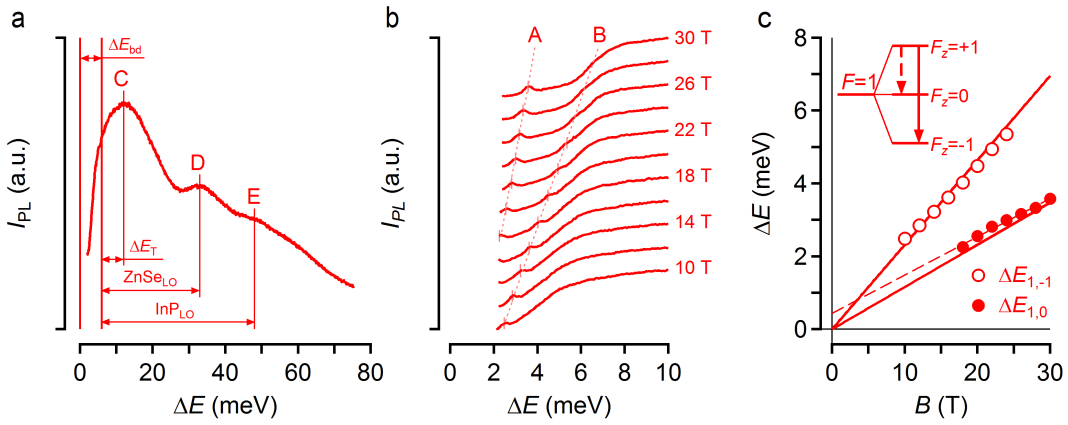


Figure 6: (a) Fluorescence line narrowing (FLN) spectrum of an ensemble of InP/ZnSe QDs excited using 2.06 eV, $\sigma^+$ polarized light. The energy difference $\Delta E$ measures the energy loss of the emitted phonons relative to 2.06 eV. Using the energy of the ZnSe and InP optical phonon as a yard stick, the indicated features are assigned to (C) acoustic phonon replica of dark state emission, (D) ZnSe LO phonon replica of dark state emission, and (E) InP LO phonon replica of dark state emission. From this analysis, we obtain a bright-dark splitting energy $\Delta E_{bd} = 6$ meV. (b) FLN spectra of the same InP/ZnSe QD ensemble in different magnetic fields as indicated. The dashed line highlights the two additional emission features, labeled A and B, that appear in the spectra, whereas the short vertical lines indicate the estimated shift of each feature relative to the excited level. (c) Energy shift of the features A and B with respect to the photo-excited $F_z = +1$ state. The full lines represent the result of a global fit to the expression of the isotropic exciton model, using $g_h$ as the only adjustable parameter ($\Delta E_{bd} = 6$ meV, $g_e = 1.6$, $g_h = -1.925$). The thin dashed line is an extrapolation of the experimental data.

strongly with increasing field strength, from 2.48 meV at 10 T to 5.35 meV at 24 T. For the largest fields, the feature is reduced to a mere shoulder on top of the rising side of the phonon-assisted dark exciton emission, making unreliable any determination of the energy shift. For both features, Figure 6c summarizes the energy shift as a function of the magnetic field, where we label the energy at which feature A and B are retrieved as $\Delta E_{1,0}$ and $\Delta E_{1,-1}$, respectively.

The observation of two emission features, shifting to lower energy with respect to the excited $F_z = +1$ bright state shows that in the absence of a magnetic field, the excited bright exciton consists of 3 different, nearly degenerate states. This result strongly contrasts to similar measurements on wurtzite CdSe QDs, which showed a bright exciton doublet.[9] We thus conclude that the spectral doublet of the single InP/ZnSe QD analyzed in Figure 3

should be seen as a nearly isotropic exciton subject to minor splitting in a singlet and a doublet state due to anisotropy along the quantization axis $z$.

For an isotropic exciton, the energy splitting $\Delta E_{1,0} = E_1 - E_0$ and $\Delta E_{1,-1} = E_1 - E_{-1}$ between the 3 bright exciton states depends on the applied magnetic field according to (see Supporting Information S5):

$$\Delta E_{1,0} = -g_h \mu_B B + \sqrt{3\eta^2 + (\eta - \frac{g_e + g_h}{2}\mu_B B)^2} - \sqrt{4\eta^2 + (\frac{g_e + g_h}{2}\mu_B B)^2} \quad (3)$$

$$\Delta E_{1,-1} = -2g_h \mu_B B + \sqrt{3\eta^2 + (\eta - \frac{g_e + g_h}{2}\mu_B B)^2} - \sqrt{3\eta^2 + (\eta + \frac{g_e + g_h}{2}\mu_B B)^2} \quad (4)$$

Here, the exchange parameter $\eta$ corresponds to a quarter of the bright-dark splitting between the high energy $F = 1$ and the low energy $F = 2$ states (see Figure 5b),[20] $g_e$ and $g_h$ are the gyromagnetic ratio of the electron and the hole, and $\mu_B$ is the Bohr magneton. In writing Eqs 3 and 4, we took as a convention that for $g_h$ positive, the energy of hole states with the angular momentum parallel to the magnetic field is lowered, whereas for $g_e$ positive, the energy of electron states with angular momentum anti-parallel to the field is lowered.[22] Unless $|g_h| \ll |g_e|$, the first term in Eqs 3 and 4 will be dominant, and a negative $g_h$ is needed to make the $F_z = +1$ state the high energy state. As shown in Supporting Information S6, keeping $\eta$ fixed at 1.5 meV yield satisfactory global fits of the experimental data to Eqs 3 and 4, yet such fits do not allow for an accurate determination of $g_e$ and $g_h$ separately. We therefore sought best fits while keeping $g_e$ fixed at values in the range $1.0 - 2.0$, which encompasses the electron $g$-factor for bulk InP and values reported for self-assembled InP-based QDs.[23] Figure 6c represents such a fit, where we took $g_e = 1.6$, a value previously reported for InP/(In,Ga)P self-assembled QDs,[23] and obtained a best fit for $g_h = -1.93 \pm 0.03$. As outlined in Supporting Information S6, sweeping $g_e$ from 1.0 to 2.0 has only a minor impact on the best fit for $g_h$, which we accordingly estimated at $g_h = -1.9 \pm 0.1$. Interestingly, this number is in reasonable agreement with the estimate of $g_h = -1.49$ we calculated using the expression proposed by Efros *et al.* (see Supporting Information S7).[20] Similarly negative

values have been predicted for multiple spherical II-VI QDs,[22] and a value of $g_h = -0.73$ was derived from Faraday rotation measurements in the case of wurtzite CdSe QDs.[24]

Looking at Figure 6c in detail, it appears that the isotropic exciton model slightly underestimates the energy splitting $\Delta E_{1,0}$ between the $F_z = +1$ and the $F_z = 0$ state. At least, a linear fit to the experimental data yields a line lying systematically higher than the global fit. This could reflect a minor splitting of the three $F = 1$ exciton states at zero field, in line with the bright exciton doublet measured on a single InP/ZnSe QD. Given the slightly larger than expected $\Delta E_{1,0}$ splitting, the low energy line of the doublet would then correspond to the $F_z = 0$ state and the high energy line to the $F_z = \pm 1$ states. Such an assignment can explain the different polarization of both lines since the $F_z = 0$ state emits linearly polarized light with an electric field along the quantization axis, whereas the $F_z = \pm 1$ states emit circularly polarized with the electric field in the $xy$ plane. Note that the particular viewing angle on a given QD can make that circularly polarized emission appears as partially linearly polarized in the detection system used, and that the phase difference between both emission lines differs from 90°. Interestingly, in the case of isotropic QDs, theoretical work indicates that the negative trion ground state emits circularly polarized light since the hole occupies either the $j_z = 3/2$ or $j_z = -3/2$ heavy hole level.[25] The positive trion, on the other hand, has a mixed ground state that leads to set of recombination pathways emitting either circular or linear polarized light.[25] Hence, the correspondence between the polarization of the high energy exciton doublet line and the trion singlet line might point towards emission from the negative trion. Such a conclusion need, however, the confirmation from a more in-depth study of these emission lines, for example to account for artefacts induced by the viewing angle on a given QD.

Both through single QD PL and FLN spectroscopy, we give evidence that radiative exciton recombination contributes to the photoluminescence of InP/ZnSe QDs. While this finding does not rule out trap-related emission pathways,[14] it does highlight that trap-related emission is not the dominant recombination process in these QDs. More in general, the

observation that excitons in InP/ZnSe QDs are nearly isotropic is far from trivial. In the case of CdSe QDs, for example, little difference was observed between the exciton fine structure of nanocrystals with a wurtzite or a zinc blende crystal structure.[26] Whereas wz-CdSe is intrinsically anisotropic, it was argued that relatively small deviations from a spherical shape can account for the similar anisotropy of the exciton in zb-CdSe QDs. Similary, an exciton model including exchange and shape anisotropy was used to describe the emission features of single zinc blende CdTe QDs.[27] Both examples suggest that deviations from an isotropic, spherical shape are to be expected in the case of colloidal QDs, and it is not clear why InP QDs should be an exception here. According to the exciton description developed by Efros, however, the impact of deviations from a spherical shape on the exciton fine structure depends on the light hole to heavy hole mass ratio $\beta = m_{lh}/m_{hh}$. Interestingly, the model predicts that the fine structure of the exciton will be insensitive to shape anisotropy when $\beta = 0.14$, which means that under such conditions also prolate or oblate ellipsoids will host isotropic excitons.[20] In the case of InP, $\beta$ depends on the direction in reciprocal space, yet an average of $\beta$ over the (100), (110) and (111) directions yields $\beta = 0.149$.[28] In contrast, for wz-CdSe, the hole mass ratio amounts to 0.28,[6] a value at which the impact of shape anisotropy on the fine structure is about maximal.[20] Possibly, having an average hole mass ratio close to the critical value of 0.14 is what makes that InP-based QDs host nearly isotropic excitons.

In summary, we have investigated the emission of InP/ZnSe QDs using a combination of cryogenic micro-photoluminescence spectroscopy of single InP/ZnSe QDs and fluorescence line narrowing spectroscopy on an ensemble of InP/ZnSe QDs. We show that the emission is related to exciton recombination, where the spectrum of a single InP/ZnSe features a bright exciton doublet, a trion singlet and a biexciton doublet. FLN spectra recorded versus magnetic field strength demonstrate that this bright exciton doublet reflects a minor deviation from the 3-fold degenerate, isotropic bright exciton expected in spherical QDs with a zinc blende structure. We assign the observation of nearly isotropic excitons in InP/ZnSe

QDs to the InP average hole mass ratio $\beta$ of 0.149. In contrast with CdSe ($\beta = 0.28$), this number is close to the value of 0.14 at which the exciton fine structure is insensitive to shape anisotropy.[20] From a fundamental perspective, isotropic excitons are highly interesting model systems for experimental studies and theory development. Different from anisotropic excitons, isotropic excitons have a fine structure solely determined by the exchange splitting. This makes the bright-dark splitting of isotropic excitons ideally suited to compare the predicted size-dependence of the exchange interaction with experimental data. In addition, the interaction between an isotropic exciton and an external field is independent of the QD orientation. As exemplified by the FLN study shown here, this makes that ensemble measurements in external fields are not compounded by orientation averaging, such that material characteristics can be determined in a direct manner from the analysis of ensembles. We therefore believe that the observation of nearly isotropic excitons in InP-based QDs opens a new direction to investigate the exciton fine structure in nanoscale semiconductors.

## Acknowledgement

Z.H, D.V.M and W.B. acknowledge support from the European Commission via the Marie-Sklodowska Curie action Phonsi (H2020-MSCA-ITN-642656). Z.H. acknowledges support by SIM-Flanders (SBO-QDOCCO), FWO-Vlaanderen (research project 17006602), and Ghent University (GOA 01G01019). F.T.R. is supported by NWO Veni grant number 722.017.002 and by The Netherlands Center for Multiscale Catalytic Energy Conversion (MCEC), an NWO Gravitation program funded by the Ministry of Education, Culture and Science of the government of The Netherlands.

## Supporting Information Available

The Supporting Information provides background on (S1) the synthesis protocol, (S2) the setup up for micro-PL analysis, (S3) the analysis of the phonon temperature, (S4) the fluo-

resecence line narrowing spectroscopy, (S5) the splitting of the isotropic exciton in a magnetic field, (S6) the fits of the FLN data to the isotropic exciton model, and (S7) an estimate of the hole $g$-factor.

# References


1. Franceschetti, A.; Zunger, A. Direct Pseudopotential Calculation of Exciton Coulomb and Exchange Energies in Semiconductor Quantum Dots. *Phys. Rev. Lett.* **1997**, *78*, 915–918.

2. Efros, A.; Rosen, M. The Electronic Structure of Semiconductor Nanocrystals. *Ann. Rev. Mat. Sci.* **2000**, *30*, 475–521.

3. Niquet, Y.; Delerue, C.; Allan, G.; Lannoo, M. Method for Tight-Binding Parametrization: Application to Silicon Nanostructures. *Phys. Rev. B* **2000**, *62*, 5109–5116.

4. Huo, Y. H.; Witek, B. J.; Kumar, S.; Cardenas, J. R.; Zhang, J. X.; Akopian, N.; Singh, R.; Zallo, E.; Grifone, R.; Kriegner, D.; Trotta, R.; Ding, F.; Stangl, J.; Zwiller, V.; Bester, G.; Rastelli, A.; Schmidt, O. G. A Light-Hole Exciton in a Quantum Dot. *Nat. Phys.* **2014**, *10*, 46–51.

5. Nirmal, M.; Norris, D. J.; Kuno, M.; Bawendi, M. G.; Efros, A. L.; Rosen, M. Observation of the "Dark Exciton" in CdSe Quantum Dots. *Phys. Rev. Lett.* **1995**, *75*, 3728–3731.

6. Norris, D. J.; Efros, A. L.; Rosen, M.; Bawendi, M. G. Size Dependence of Exciton Fine Structure in CdSe Quantum Dots. *Phys. Rev. B* **1996**, *53*, 16347–16354.

7. Labeau, O.; Tamarat, P.; Lounis, B. Temperature Dependence of the Luminescence Lifetime of Single CdSe/ZnS Quantum Dots. *Phys. Rev. Lett.* **2003**, *90*, 257404.

8. Biadala, L.; Louyer, Y.; Tamarat, P.; Lounis, B. Direct Observation of the Two Lowest

Exciton Zero-Phonon Lines in Single CdSe/ZnS Nanocrystals. *Phys. Rev. Lett.* **2009**, *103*, 037404.

9. Furis, M.; Htoon, H.; Petruska, M. A.; Klimov, V. I.; Barrick, T.; Crooker, S. A. Bright-Exciton Fine Structure and Anisotropic Exchange in CdSe Nanocrystal Quantum Dots. *Phys. Rev. B* **2006**, *73*, 241313.

10. Htoon, H.; Furis, M.; Crooker, S. A.; Jeong, S.; Klimov, V. I. Linearly Polarized 'Fine Structure' of the Bright Exciton State in Individual CdSe Nanocrystal Quantum Dots. *Phys. Rev. B* **2008**, *77*, 035328.

11. Granados del Aguila, A.; Pettinari, G.; Groeneveld, E.; de Mello Donega, C.; Vanmaekelbergh, D.; Maan, J. C.; Christianen, P. C. M. Optical Spectroscopy of Dark and Bright Excitons in CdSe Nanocrystals in High Magnetic Fields. *J. Phys. Chem. C* **2017**, *121*, 23693–23704.

12. Biadala, L.; Siebers, B.; Beyazit, Y.; Tessier, M. D.; Dupont, D.; Hens, Z.; Yakovlev, D. R.; Bayer, M. Band-Edge Exciton Fine Structure and Recombination Dynamics in InP/ZnS Colloidal Nanocrystals. *ACS Nano* **2016**, *10*, 3356–3364.

13. Brodu, A.; Ballottin, M. V.; Buhot, J.; van Harten, E. J.; Dupont, D.; La Porta, A.; Prins, P. T.; Tessier, M. D.; Versteegh, M. A. M.; Zwiller, V.; Bals, S.; Hens, Z.; Rabouw, F. T.; Christianen, P. C. M.; de Mello Donega, C.; Vanmaekelbergh, D. Exciton Fine Structure and Lattice Dynamics in InP/ZnSe Core/Shell Quantum Dots. *ACS Photonics* **2018**, *5*, 3353–3362.

14. Janke, E. M.; Williams, N. E.; She, C.; Zherebetskyy, D.; Hudson, M. H.; Wang, L.; Gosztola, D. J.; Schaller, R. D.; Lee, B.; Sun, C.; Engel, G. S.; Talapin, D. V. Origin of Broad Emission Spectra in InP Quantum Dots: Contributions from Structural and Electronic Disorder. *Journal of the American Chemical Society* **2018**, *140*, 15791–15803.

15. Cui, J.; Bayler, A. P.; Marshall, L. F.; Chen, O.; Harris, D. K.; Wanger, D. D.; Brokmann, X.; Bawendi, M. G. Direct Probe of Spectral Inhomogeneity Reveals Synthetic Tunability of Single-Nanocrystal Spectral Linewidths. *Nat. Chem.* **2013**, *5*, 602–606.

16. Chandrasekaran, V.; Tessier, M. D.; Dupont, D.; Geiregat, P.; Hens, Z.; Brainis, E. Nearly Blinking-Free, High-Purity Single-Photon Emission by Colloidal InP/ZnSe Quantum Dots. *Nano Letters* **2017**, *17*, 6104–6109.

17. Tessier, M. D.; Dupont, D.; De Nolf, K.; De Roo, J.; Hens, Z. Economic and Size-Tunable Synthesis of InP/ZnE (E = S, Se) Colloidal Quantum Dots. *Chem. Mater.* **2015**, *27*, 4893–4898.

18. Talati, M.; Jha, P. K. Acoustic Phonons in Semiconductor Nanocrystals. *Comp. Mat. Sci.* **2006**, *37*, 58–63.

19. Fernée, M. J.; Littleton, B. N.; Rubinsztein-Dunlop, H. Detection of Bright Trion States Using the Fine Structure Emission of Single CdSe/ZnS Colloidal Quantum Dots. *ACS Nano* **2009**, *3*, 3762–3768.

20. Efros, A. L.; Rosen, M.; Kuno, M.; Nirmal, M.; Norris, D. J.; Bawendi, M. Band-Edge Exciton in Quantum Dots of Semiconductors with a Degenerate Valence Band: Dark and Bright Exciton States. *Phys. Rev. B* **1996**, *54*, 4843–4856.

21. Barak, Y.; Meir, I.; Shapiro, A.; Jang, Y.; Lifshitz, E. Fundamental Properties in Colloidal Quantum Dots. *Adv. Mater.* **2018**, *30*, 1801442.

22. Shornikova, E. V.; Biadala, L.; Yakovlev, D. R.; Feng, D.; Sapega, V. F.; Flipo, N.; Golovatenko, A. A.; Semina, M. A.; Rodina, A. V.; Mitioglu, A. A.; Ballottin, M. V.; Christianen, P. C. M.; Kusrayev, Y. G.; Nasilowski, M.; Dubertret, B.; Bayer, M. Electron and Hole g-Factors and Spin Dynamics of Negatively Charged Excitons in CdSe/CdS Colloidal Nanoplatelets with Thick Shells. *Nano Letters* **2018**, *18*, 373–380.

23. Syperek, M.; Yakovlev, D. R.; Yugova, I. A.; Misiewicz, J.; Jetter, M.; Schulz, M.; Michler, P.; Bayer, M. Electron and Hole Spins in InP/(Ga,In)P Self-Assembled Quantum Dots. *Phys. Rev. B* **2012**, *86*, 125320.

24. Gupta, J. A.; Awschalom, D. D.; Efros, A. L.; Rodina, A. V. Spin Dynamics in Semiconductor Nanocrystals. *Phys. Rev. B* **2002**, *66*, 125307.

25. Shabaev, A.; Rodina, A. V.; Efros, A. L. Fine Structure of the Band-Edge Excitons and Trions in CdSe/CdS Core/Shell Nanocrystals. *Phys. Rev. B* **2012**, *86*, 205311.

26. Moreels, I.; Raino, G.; Gomes, R.; Hens, Z.; Stoferle, T.; Mahrt, R. F. Band-Edge Exciton Fine Structure of Small, Nearly Spherical Colloidal CdSe/ZnS Quantum Dots. *ACS Nano* **2011**, *5*, 8033–8039.

27. Tilchin, J.; Rabouw, F. T.; Isarov, M.; Vaxenburg, R.; Van Dijk-Moes, R. J. A.; Lifshitz, E.; Vanmaekelbergh, D. Quantum Confinement Regimes in CdTe Nanocrystals Probed by Single Dot Spectroscopy: From Strong Confinement to the Bulk Limit. *ACS Nano* **2015**, *9*, 7840–7845.

28. Kim, Y.-S.; Hummer, K.; Kresse, G. Accurate Band Structures and Effective Masses for InP, InAs, and InSb Using Hybrid Functionals. *Phys. Rev. B* **2009**, *80*, 035203.

# Graphical TOC Entry